Tellus (1981), *33*, 402–410

Frictional influence on internal Kelvin waves

By EIVIND A. MARTINSEN, *Mechanics Department, University of Oslo, P.O. Box 1053, Blindern, Oslo 3, Norway*, and JAN ERIK WEBER, *Institute of Geophysics, University of Oslo, P.O. Box 1022, Blindern, Oslo 3, Norway.*

(Manuscript received May 20; in final form September 4, 1980)

ABSTRACT

Frictional influence on free internal Kelvin waves is studied theoretically. For continuous stratification the friction enters as an eddy viscosity, and the solutions are written in terms of normal modes. This approach implies a stress-free bottom. To obtain an analytical solution, we have assumed that the vertical variation of the eddy viscosity is inversely proportional to the square of the Brunt-Väisälä frequency. Coastal as well as equatorial Kelvin waves are considered. The effects of bottom friction and frictional drag at an interface are studied explicitly in a vertically integrated two-layer model, taking the shear stress at a boundary to be proportional to the velocity difference across it. Formally, the continuously stratified case and the two-layer model result in the same set of equations. Explicit formulae for the frictional damping in time, the Rossby radius of deformation, the frequency, the phase difference between velocity and elevation, and the tilting of the internal co-phase lines backwards from the coast are given. In particular, the latter effect is shown to be much stronger for baroclinic waves than for the barotropic mode of the same wavelength.

1. Introduction

The fact that friction significantly modifies long barotropic waves in a shallow sea has been known for a long time. Sverdrup (1927) and Fjeldstad (1929) analyzed the semi-diurnal tides on the North Siberian Shelf as barotropic inertial-gravity waves subject to eddy viscosity. Features such as reduced phase speed, decreasing amplitude as the waves progress and phase lag between maximum current and high water were found to result from the effect of friction. Also vertical variation of the tidal currents due to Ekman layers at the bottom (and top, when ice covered) was demonstrated.

Fjeldstad (1929) considered barotropic Kelvin waves as well, assuming that the bottom friction was proportional to the mean velocity. In particular he demonstrated that friction makes the co-tidal lines slant backwards from the coast. Brink and Allen (1978) find a similar effect for barotropic vorticity waves on a sloping continental shelf. Recently Mofjeld (1980) has applied Sverdrup's (1927) solution to barotropic Kelvin waves, assuming a constant eddy viscosity and a no-slip bottom.

It is clear that friction affects internal waves more strongly than barotropic waves (Fjeldstad, 1964). However, it appears that a discussion of frictional effects on internal Kelvin waves is lacking, and this has motivated the present study.

First we consider a model with continuous stratification. The solutions are written in terms of normal modes (Lighthill, 1969). This approach implies a stress-free bottom. Accordingly, the formulation is most applicable to a relatively deep ocean. Analytical solutions for the internal Kelvin modes are presented, and explicit formulae for the frictional damping, Rossby radius of deformation, frequency, phase difference, and tilting of internal co-phase lines are given. Also equatorial internal Kelvin waves are considered.

To study the effects of bottom friction and frictional drag at an interface, we choose a vertically integrated two-layer model. Since our primary interest is the qualitative influence of friction on free waves, and not the detailed structure of the motion within a thin Ekman layer at the bottom, we take the bottom stress to be proportional to the mean velocity. However, a numerical analysis for the barotropic mode with a

0040-2826/81/040402-09$02.50/0

bottom stress proportional to the square of the velocity is shown to yield quantitatively the same results as those obtained with a linear bottom stress. The same assumption is made at the interface where the drag is taken to be proportional to the velocity difference. By utilizing the formal identity between the continuously stratified case and the two-layer model, analytical solutions are presented also for the latter problem.

2. Effect of internal friction

2.1. *Coastal waves*

Consider a semi-infinite ocean of constant depth H and bounded by a straight coast line. We choose a Cartesian coordinate system (x,y,z) such that the origin is situated at the undisturbed surface, the x-axis points along the coast, with the sea at $y \geq 0$. The z-axis is positive upwards. Consider the theory of internal waves in a rotating frame of reference. The fluid is incompressible, and the waves result from small perturbations from a state of rest characterized by a horizontally-uniform, stable stratification, $\rho(z)$. We assume that the typical wavelengths are much larger than the depth of the layer, so that the pressure to a good approximation can be taken as hydrostatic. Along the surface there is no variation of pressure. With the aid of the Boussinesq approximation, the governing equations are those of Gill and Clarke (1974).

The variables may be separated into normal modes (Lighthill, 1969), and the reader is referred to Gill and Clarke (1974) for details. We assume that

$$\vec{v} = \sum_{n=0}^{\infty} \vec{v}_n(x,y,t)\,\phi_n'(z)$$

$$p = \sum_{n=0}^{\infty} p_n(x,y,t)\,\phi_n'(z)$$

$$\zeta = \sum_{n=0}^{\infty} \zeta_n(x,y,t)\,\phi_n(z) \tag{2.1}$$

where $\vec{v}(=u,v)$ is the horizontal perturbation velocity, p the perturbation pressure and ζ the vertical displacement of the isopycnals. The prime denotes derivative with respect to z. The eigenfunctions ϕ_n are solutions of

$$\phi_n'' + \frac{N^2}{c_n^2}\phi_n = 0 \tag{2.2}$$

subject to the boundary conditions

$$\phi_n' - \frac{g}{c_n^2}\phi_n = 0, \quad z = 0$$
$$\phi_n = 0, \quad z = -H. \tag{2.3}$$

Here N is the Brunt-Väisälä frequency defined by

$$N^2 = -\frac{g}{\rho_0}\frac{\partial \rho(z)}{\partial z}$$

where g is the acceleration due to gravity, and ρ_0 is a constant reference density. Accordingly, for a specified $N = N(z)$, (2.2) and (2.3) yield the eigenvalues c_n. Furthermore we have that $p_n = c_n^2\,\zeta_n$. It is easily shown that the functions ϕ_n' form an orthogonal set, and they are conveniently normalized by

$$\int_{-H}^{0} (\phi_n')^2\,dz = H. \tag{2.4}$$

Utilizing the orthogonality property, the governing equations may be written

$$\frac{\partial u_n}{\partial t} - fv_n = -c_n^2\frac{\partial \zeta_n}{\partial x} + \tau_n^{(x)}$$
$$\frac{\partial v_n}{\partial t} + fu_n = -c_n^2\frac{\partial \zeta_n}{\partial y} + \tau_n^{(y)}$$
$$\frac{\partial \zeta_n}{\partial t} = -\frac{\partial u_n}{\partial x} - \frac{\partial v_n}{\partial y} \tag{2.5}$$

where $n = 0,1,2 \ldots$. Furthermore, f is the constant Coriolis parameter, t denotes time and

$$\tau_n^{(x)} = \frac{1}{\rho_0 H}\int_{-H}^{0}\frac{\partial \tau^{(x)}}{\partial z}\phi_n'\,dz$$
$$\tau_n^{(y)} = \frac{1}{\rho_0 H}\int_{-H}^{0}\frac{\partial \tau^{(y)}}{\partial z}\phi_n'\,dz \tag{2.6}$$

where $\tau^{(x)}$ and $\tau^{(y)}$ are the stress components in the x- and y-directions, respectively.

The boundary condition at the coast is

$$v_n = 0, \quad \text{at } y = 0. \tag{2.7}$$

The above formulation has been applied to investigate the response of a stratified ocean to atmospheric forcing (Lighthill, 1969; Csanady, 1972; Gill and Clarke, 1974; Röed; 1979). In such cases the stress distribution is usually taken to be a known function of depth. In the present paper we are concerned with the effect of friction on free waves. To model this, we use the concept of eddy viscosity. Assuming the vertical variation to be much larger than the horizontal, we take

$$\tau^{(x)} = \mu \frac{\partial u}{\partial z}$$
$$\tau^{(y)} = \mu \frac{\partial v}{\partial z} \tag{2.8}$$

where μ is the dynamic eddy coefficient. By inserting from (2.1) into (2.8) and applying (2.2) and (2.3), we see that the present formulation leads to $\tau^{(x)} = \tau^{(y)} = 0$ at $x = -H$, i.e. a stress-free bottom. However, with reference to the two-layer model to be discussed in the next section, it is seen that the effect of bottom friction tends to vanish when the depth of the lower layer becomes large. Accordingly, the formulation in this section probably is most applicable to a relatively deep ocean.

Since the density difference between the atmosphere and the ocean is so much greater than density differences within the ocean, one mode has quite a different character from all the others. This is the barotropic mode ($n = 0$), for which, to a good approximation (Gill and Clarke, 1974)

$$\phi_0 = z + H$$
$$c_0 = \sqrt{gH} \tag{2.9}$$

and accordingly, $\tau_0^{(x)} = \tau_0^{(y)} = 0$. From (2.5) and (2.7) we then see that the barotropic mode, in the absence of bottom friction, propagates as an undamped Kelvin wave with the coast to the right (on the Northern hemisphere) with the velocity $c_0 = \sqrt{gH}$.

For the remaining baroclinic modes ($n = 1, 2, 3 \ldots$), the boundary condition at the surface can, to a good approximation, be taken as $\zeta = 0$, or $\phi_n(0) = 0$ (the rigid lid approximation). In general, with a variable kinematic eddy viscosity $\nu = \mu/\rho_0$ and a variable Brunt-Väisälä-frequency N, the equations (2.5) do not decouple, since, from (2.6), $\tau_n^{(x)} = \tau_n^{(x)}(u_1, u_2, \ldots)$ and $\tau_n^{(y)} = \tau_n^{(y)}(v_1, v_2, \ldots)$. To simplify the problem, however, we assume that $\nu N^2 =$ constant, which in many cases seem to be a reasonable assumption (Fjeldstad, 1964). Then the system of equations for the baroclinic modes ($n = 1, 2, 3 \ldots$) do decouple, and we obtain

$$\frac{\partial u_n}{\partial t} - f v_n = -c_n^2 \frac{\partial \zeta_n}{\partial x} - K_n u_n$$
$$\frac{\partial v_n}{\partial t} + f u_n = -c_n^2 \frac{\partial \zeta_n}{\partial y} - K_n v_n$$
$$\frac{\partial \zeta_n}{\partial t} = -\frac{\partial u_n}{\partial x} - \frac{\partial v_n}{\partial y} \tag{2.10}$$

where $K_n = \nu N^2/c_n^2$. The boundary conditions are

$$v_n = 0, \quad y = 0 \tag{2.11a}$$
$$u_n = v_n = \zeta_n \to 0, \quad y \to \infty \tag{2.11b}$$

We note that the system of equations (2.10) formally is identical to that obtained for long inertial-gravity waves in a homogeneous layer where the bottom friction is proportional to the mean velocity; see also sec. 3 of the present paper.

We assume wave solutions of the form

$$u_n, v_n, \zeta_n = \{u_n(y), v_n(y), \zeta_n(y)\} \exp(ikx + \omega_n t) \tag{2.12}$$

where k is a real wave number in the x-direction and ω_n is the complex growth rate. From (2.10) we then obtain for v_n:

$$v_n(y) = C_1 e^{\kappa y} + C_2 e^{-\kappa y}.$$

Here C_1, C_2 are constants and

$$\kappa^2 = \frac{\omega_n}{(\omega_n + K_n)c_n^2} \{f^2 + K_n^2 + c_n^2 k^2 + \omega_n) + 2\omega_n K_n + c_n^2 k^2 K_n/\omega_n\}$$

which is generally complex and non-zero. From (2.11a) we obtain $C_2 = -C_1 \equiv C$, while (2.11b) implies $C = 0$. Hence v_n vanishes everywhere.

Utilizing this fact, and also that the governing equations for the internal modes are formally identical to those for the barotropic surface mode, we may proceed as Fjeldstad (1929). We shall, however, adopt a slightly different approach. In particular we shall avoid using a wave component with an amplitude that varies exponentially in x, since the ocean is assumed unlimited in the direction along the coast. Therefore solutions of the type (2.12) will be considered. By introducing (2.12) into (2.10), and utilizing that $v_n = 0$, we find for the growth rate

$$\omega_n = -K_n/2 - kc_n(1 - K_n^2/4k^2 c_n^2)^{1/2} i, \tag{2.13}$$

where only the minus sign is kept in the imaginary part. This is done in order that the solutions shall remain finite when $y \to \infty$. We note that (2.13) formally is identical to that obtained for long waves in a non-rotating channel (Defant, 1951, p. 156).

We observe from (2.13) that the mode in questions will be purely damped in time if $K_n > 2kc_n$. Hence, in terms of the wavelength $\lambda = 2\pi/k$, the n^{th} internal mode will lose its character as a travelling wave if $\lambda > \lambda_c$, where

$$\lambda_c = \frac{4\pi c_n^3}{\nu N^2}. \tag{2.14}$$

Letting the real part represent the physical solution, we obtain from (2.10)

$$\begin{aligned} u_n &= A_n \exp(-K_n t/2 - y/a_n) \cos(kx + l_n y - \sigma_n t) \\ \zeta_n &= (A_n/c_n) \exp(-K_n t/2 - y/a_n) \\ &\quad \times \cos(kx + l_n y - \sigma_n t + \gamma_n) \end{aligned} \tag{2.15}$$

where A_n is a real constant. Furthermore, the Rossby radius of deformation a_n, the wavenumber in the y-direction l_n, the frequency σ_n and the phase difference γ_n are defined by

$$\begin{aligned} a_n &= \frac{c_n}{f(1 - K_n^2/4c_n^2 k^2)^{1/2}} \\ l_n &= \frac{fK_n}{2c_n^2 k} \\ \sigma_n &= kc_n(1 - K_n^2/4c_n^2 k^2)^{1/2} \\ \gamma_n &= \arctan(K_n/2\sigma_n) \end{aligned} \tag{2.16}$$

Each internal mode is seen to constitute a progressive wave, trapped to the coast, with an amplitude that decreases exponentially in time. The alongshore wave component propagates with the coast to the right (on the northern hemisphere) like barotropic Kelvin waves in the absence of friction. We note, however, that effect of friction introduces an additional wave component normal to the coast, such that the wave vector, or the direction of propagation of the wave, forms an angle $\alpha_n = \arctan(l_n/k)$ with the coast. By insertion from (2.16), we obtain

$$\alpha_n = \arctan(fN^2 \nu/2c_n^4 k^2) \tag{2.17}$$

This means that the lines of constant phase, or the internal co-phase lines, are not normal to the coast, but slope backwards. We note that this effect becomes progressively stronger for higher internal modes. The tilting of co-phase lines due to friction has been noted by Fjeldstad (1929) and Mofjeld (1980) for barotropic Kelvin waves. A similar effect was found by Brink and Allen (1978) for barotropic vorticity waves on a sloping continental shelf.

Since $K_n = \nu N^2/c_n^2$, we see, as expected, that higher modes become progressively more damped. We also find that friction leads to an increase of the Rossby radius of deformation and a decrease of wave frequency for the internal modes.

As noted by Sverdrup (1927) for barotropic waves in the open ocean, and by Fjeldstad (1929) for barotropic Kelvin waves, we find that friction also in the baroclinic case causes a phase lag between the current and the vertical displacement of the isopycnals (maximum elevation occurs after maximum current for the mode in question). From (2.16) we observe that this phase difference becomes progressively larger for higher modes.

The above results have been derived under the assumption νN^2 = const. However, the present approach also works for more general cases, but then eqs. (2.5) must be solved numerically.

As a simple example we may take N = constant and ν = constant throughout the layer. It is then straightforward to show from (2.2), with boundary conditions $\phi_n = 0$ at $z = 0$, which is a very good approximation for baroclinic modes (Gill and Clarke, 1974), and $\phi_n = 0$ at $z = -H$, that $c_n = NH/n\pi$, $n = 1, 2, \ldots$. Hence

$$\alpha_n = \arctan\left(\frac{\pi^2}{8} \frac{\nu f \lambda^2}{N^2 H^4} n^4\right) \tag{2.18}$$

Taking $N = 10^{-3}\ \text{s}^{-1}$, $\nu = 10^{-3}\ \text{m}^2/\text{s}$, $f = 10^{-4}\ \text{s}^{-1}$, $H = 700$ m and $\lambda = 10^3$ km, we obtain for the first four modes

$$\begin{aligned} &\alpha_1 = 27.2°, \quad \alpha_2 = 83.1°, \quad \alpha_3 = 88.6°, \\ &\alpha_4 = 89.6°. \end{aligned} \tag{2.19}$$

We thus see that the baroclinic modes from the second on propagate in a direction almost normal to the coast.

By utilizing (2.16), we find that the phase difference γ_n between maximum current and maximum elevation for these modes are quite small, being 0.002π, 0.02π, 0.06π and 0.2π, respectively.

In the same example the characteristic decay time, T_n, is

$$T_n = \frac{1}{K_n/2} = \frac{2H^2}{\nu n^2 \pi^2} \tag{2.20}$$

which yields

$$T_1 = 1149 \text{ days}, \quad T_2 = 287 \text{ days} \quad T_3 = 128 \text{ days}, \quad T_4 = 72 \text{ days} \tag{2.21}$$

From this we note the interesting fact that, although the damping in time due to internal friction may be quite small for baroclinic Kelvin waves, the direction of propagation of the waves is significantly altered by the presence of friction.

From the discussion of the growth rate (2.13) we find that the nth baroclinic mode will be purely damped in time, and hence lose its character as a progressive wave, if $n > (4NH^3/\pi^2 \nu\lambda)^{1/3}$. With the values of the parameters used in the present example, this occurs for $n > 5$. For these modes also the Rossby radius of deformation is purely imaginary, so there is no trapping to the coast.

2.2. *Equatorial waves*

Results for baroclinic equatorial Kelvin waves follow readily from the analysis in *sec. 2.1*. We let the x-axis be directed eastwards along the equator with the y-axis pointing northwards and the origin at the equator. Let $f = \beta y$ in (2.10), where $\beta > 0$. The dispersion relation (2.13) is independent of f and becomes the same as before. By utilizing the definition of the frequency σ_n in (2.16), the solution for the baroclinic velocity modes may be written

$$u_n = A_n \exp(-K_n t/2 - y^2/a_n^2) \cos\left(kx + \frac{\beta K_n}{4kc_n^2} y^2 - \sigma_n t\right) \tag{2.22}$$

being valid at both sides of the equator. A similar expression with a phase lag, may be derived for the vertical displacement ζ_n.

The Rossby radius of deformation is now

$$a_n = \left(\frac{2kc_n^2}{\beta\sigma_n}\right)^{1/2} \tag{2.23}$$

while the form of the internal co-phase lines is governed by

$$x = \frac{-\beta K_n}{4k^2 c_n^2} y^2 + \text{const.} \tag{2.24}$$

This equation describes parabolas with axes along the equator. We thus see that internal friction makes the co-phase lines curve westwards on both sides of the equator.

3. A two-layer model

To investigate the effect of bottom friction and frictional drag at an interface on internal Kelvin waves in the simplest way, we let the density distribution be approximated by a two-layer model with upper and lower layers of depths H_1, H_2, and uniform densities ρ_1, ρ_2, respectively. We assume again that the typical wave-lengths are much larger than the depth of the layers, so that the pressure to a good approximation can be taken as hydrostatic. Instead of proceeding as in the previous section, we now integrate the linearized equations vertically in each layer, assuming that there is no atmospheric forcing at the surface. When the density difference between the layers, $\Delta\rho = \rho_2 - \rho_1$, is sufficiently small, the equations governing the internal mode may be written

$$\begin{aligned} \frac{\partial U}{\partial t} - fV &= -c_1^2 \frac{\partial \zeta}{\partial x} - KU \\ \frac{\partial V}{\partial t} + fU &= -c_1^2 \frac{\partial \zeta}{\partial y} - KV \\ \frac{\partial \zeta}{\partial t} &= -\frac{\partial U}{\partial x} - \frac{\partial V}{\partial y} \end{aligned} \tag{3.1}$$

where U, V are the vertically integrated velocities in the lower layer. (The fluxes in the upper layer have equal magnitude, but opposite signs). ζ denotes the vertical displacement of the interface. The parameter c_1 is the velocity of free internal waves in the absence of rotation and friction, i.e.

$$c_1 = \left\{\frac{g\Delta\rho H_1 H_2}{\rho_2(H_1 + H_2)}\right\}^{1/2} \tag{3.2}$$

The friction parameter K contains bottom friction as well as drag from the upper layer. We have assumed for simplicity that the stress components $\tau^{(x)}$, $\tau^{(y)}$ at a boundary are proportional to the relative velocity across it. At the interface; $\tau^{(x)} = \rho_2 r'(u_1 - u_2)$, while at the bottom $\tau^{(x)} = \rho_2 r u_2$, where u_1 and u_2 are the mean velocities in the upper and lower layers, respectively; see also Bennett (1978). Similar expressions are assumed for the y-components. With these assumptions, it follows that K for the internal mode may be written

$$K = \frac{rH_1}{H_2(H_1 + H_2)} + \frac{r'(H_1 + H_2)}{H_1 H_2} \tag{3.3}$$

where the first part represents bottom friction and the second internal friction. We observe that the effect of bottom friction on the internal mode tends to vanish when $H_2 \to \infty$, which justifies the previous assumption of a stress-free bottom in the continuously stratified deep ocean case. We also note, as pointed out before, that eqs. (3.1) formally are identical to those for the barotropic mode, provided $c_1 \to c_0 = \sqrt{g(H_1 + H_2)}$ and $K \to K_0 = r_0/(H_1 + H_2)$.

Eqs. (3.1) also have the same form as those for the baroclinic modes (2.10). With $V = 0$ everywhere, which follows from the proof in the *sec. 2.1*, the solution for the internal Kelvin mode may be written

$$U = A \exp(-Kt/2 - y/a) \cos(kx + ly - \sigma t)$$
$$\zeta = (A/c_1) \exp(-Kt/2 - y/a) \cos(kx + ly - \sigma t + \gamma) \tag{3.4}$$

where

$$a = c_1/f(1 - K^2/4c_1^2 k^2)^{1/2}$$
$$l = fK/2c_1^2 k$$
$$\sigma = kc_1(1 - K^2/4c_1^2 k^2)^{1/2}$$
$$\gamma = \arctan(K/2\sigma)$$

and where K is given by (3.3).

The tilt of the internal co-phase lines backwards from the direction normal to the coast is given by

$$\alpha = \arctan(fK/2\sigma_1^2) \tag{3.6}$$

where $\sigma_1 = kc_1$ is the frequency of internal Kelvin waves in the absence of friction.

Proper values for the friction coefficients r, r' in (3.3) are not easy to assess. For the barotropic surge in a shallow sea like the North Sea, the friction coefficient r_0 has been estimated to 0.0024 m/s in computations by Heaps (1969) and Timmerman (1977). This results in good agreement between theory and observations (Timmerman, 1977). Now, values for the coefficients in the internal case are more difficult to estimate, and in the following attempt we use hydrographic data which may be typical for a coastal shelf area. First, by using the fact that the fluxes in the two layers are of equal magnitude and of opposite signs, the magnitude of the maximum velocity difference across the interface, Δu, may be written

$$\Delta u = b\left(\frac{g\Delta\rho}{\rho}\right)^{1/2} \left(\frac{H_1 + H_2}{H_1 H_2}\right)^{1/2} \tag{3.7}$$

where $b(=A/c_1$ in 3.4) is the amplitude of the internal elevation. By taking $H_1 = 20$ m, $H_2 = 200$ m, $b = 10$ m and $\Delta\rho/\rho = 10^{-3}$, we find that $\Delta u = 0.2$ m/s. Accordingly perturbations of sufficiently small wavelength, here less than 17 m, will grow (Kelvin-Helmholtz instability), leading to a turbulent interfacial layer. Taking the thickness of this layer to be Δz, we assume that the shear-stress at the interface can be written

$$\tau^{(x)} = \mu\Delta u/\Delta z = \rho r' \Delta u \tag{3.8}$$

Introducing the gradient Richardson number, $Ri = (g/\rho)(\Delta\rho/\Delta z)/(\Delta u/\Delta z)^2$, we obtain from (3.7) and (3.8) that

$$r' = \left(\frac{\nu}{Ri}\right) \frac{H_1 H_2}{b^2(H_1 + H_2)} \tag{3.9}$$

where ν is the kinematic eddy viscosity. Assuming the interfacial layer to be in a marginal turbulent state, i.e. Ri of order unity, and taking $\nu \sim 10^{-3}$ m²/s, we obtain $r' = 1.8 \cdot 10^{-4}$ m/s. This is more than a factor 10 higher than the value used by Bennett (1978) for numerical simulations in Lake Ontario. However, the uncertainty in this sort of estimate is quite large, and we stick to the value derived here.

From (3.3) we note that r must be a factor of 100 greater than r' for the bottom term to be comparable with that arising from the drag at the interface in this example. Even with the small value of r' ($=1.0 \cdot 10^{-5}$ m/s) used by Bennett (1978), this would imply that r had to be of the same order of magnitude as r_0 for the barotropic mode, which we consider as highly unrealistic. Hence the contribution from bottom friction to K in (3.3) can be neglected in this case. With the values above, we find a critical wavelength in the x-direction of about 540 km. For wavelengths larger than this, the motion will be purely damped in time. In the present example, we choose $\lambda \equiv 2\pi/k = 100$ km and $f = 1.2 \cdot 10^{-4}$ s⁻¹. We then obtain for the tilting of the internal co-phase lines that $\alpha = 40°$. The phase difference, γ, between current and elevation is 0.06 π and the Rossby radius of deformation, $a = 3.6$ km. The corresponding values for the barotropic surface mode of the same wavelength are found to be $\alpha \approx \gamma \approx 0$, and $a = 392$ km. This again emphasizes the strong frictional effect on the direction of propagation of internal Kelvin waves. As pointed out before one should keep in mind that there is quite a lot of uncertainty involved in these estimates. If one, for example, applies the value of the friction coefficient r' at the interface used by Bennett (1978), the tilt angle would be reduced to 3°. If one considers the semi-diurnal barotropic tide as a generating mechanism, i.e. take $\sigma_1 = 2\pi/(12\text{ h})$ in (3.6), we obtain, with $r' = 1.8 \cdot 10^{-4}$ m/s, a tilt angle of 2°.

Finally we note that the decay time in this case is about 56 h. This is very much smaller than the decay time for the first modes in a continuously stratified ocean; see (2.21). One should bear in mind, however, that the density stratification in the two cases is completely different so they cannot really be compared.

4. A numerical example

Since the equations for the free internal mode in a two-layer model formally are identical to those for the barotropic mode in a homogeneous sea, we have chosen to demonstrate numerically the effect of bottom friction in the latter case. The geometry is given in Fig. 1. The numerical finite-difference scheme is described elsewhere (Martinsen et al. 1979), where also the boundary conditions at the coast as well as in the open sea are discussed. As a simplified model for the meteorological forcing, we take into consideration only the wind stress acting parallel to the coast. This situation is in fact most efficient in generating Kelvin waves; see Gjevik and Røed (1976). Assuming a steady wind field, we take the wind-stress components as

$$\tau^{(x)} = \tau_0 \exp(-p^2(x-x_0)^2 - qy)$$
$$\tau^{(y)} = 0 \qquad (4.1)$$

Here $(x_0,0)$ is the position of the wind-stress

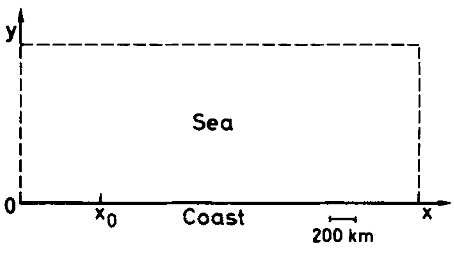

Fig. 1. The geometry of the numerical model. Broken lines are boundaries in the open-sea. The origin is at 0, and x_0 denotes the position of the wind-stress maximum.

maximum τ_0, while p and q give the decay in the x- and y-direction, respectively. In the numerical simulation we used $p^{-1} = 540$ km, $q^{-1} = 180$ km, $x_0 = 600$ km and $\tau_0 = 2.3$ kg/ms^2, corresponding to a maximum wind of about 25 m/s. The other parameters are the depth, $H = 50$ m, the Coriolis parameter, $f = 1.2 \cdot 10^{-4}$ s^{-1}; the acceleration of gravity, $g = 9.8$ m/s^2 and the friction coefficient, $K = r_0/H = 4.8 \cdot 10^{-5}$ s^{-1}. The space and time steps in the computations were 20 km and 240 s, respectively.

The simulated motion starts from rest. Then the wind stress (4.1) is switched on. In Fig. 2(a) we have displayed the isolines for the surface elevation after 8 h. The generated surge is a result of the divergence of the wind stress and the Ekman transport normal to the coast. The wind stress is then switched off, and Fig. 2(b) gives the situation 4 h later. The surge still has some reminiscences of the generation process, but also shows features of Kelvin wave behaviour. In Figs. 2(c) and 2(d), corresponding to 12 and 16 h after the stress was switched off, the surge consists mainly of free Kelvin waves. The role of bottom friction is clearly demonstrated by the twisting of the shape of the isolines, and the decay in amplitude as the surge progresses. For comparison, and also for presenting a clearer picture of these features, we consider a single barotropic Kelvin mode. This is obtained from the analytical solution (3.4) by choosing $c_1 = \sqrt{gH}$ and $K = r_0/H$, where r_0 and H have the same value as in the numerical example. The wavelength is taken to be 2160 km, which roughly equals twice the width of the free surge in Figs. 2(c) and 2(d). The result is plotted in Fig. 3(a), where the maximum amplitude is approximately the same as for the surge in Fig. 2(c), while Fig. 3(b) depict the situation 4 h later. The striking similarity between the isolines of the free surge and the analytical Kelvin mode should be noted. In the analytical example in Figs. 3(a) and 3(b) the lines of constant phase are tilted 35° backwards from the normal to the coast. At a fixed point on the coast maximum current will occur 2 h before high water in this case.

We have also performed numerical computations where we assumed that the bottom stress was proportional to the square of the mean velocity. The results showed backward tilting of the co-tidal lines and amplitude decrease, and qualitatively agreed with those presented here for linear bottom friction.

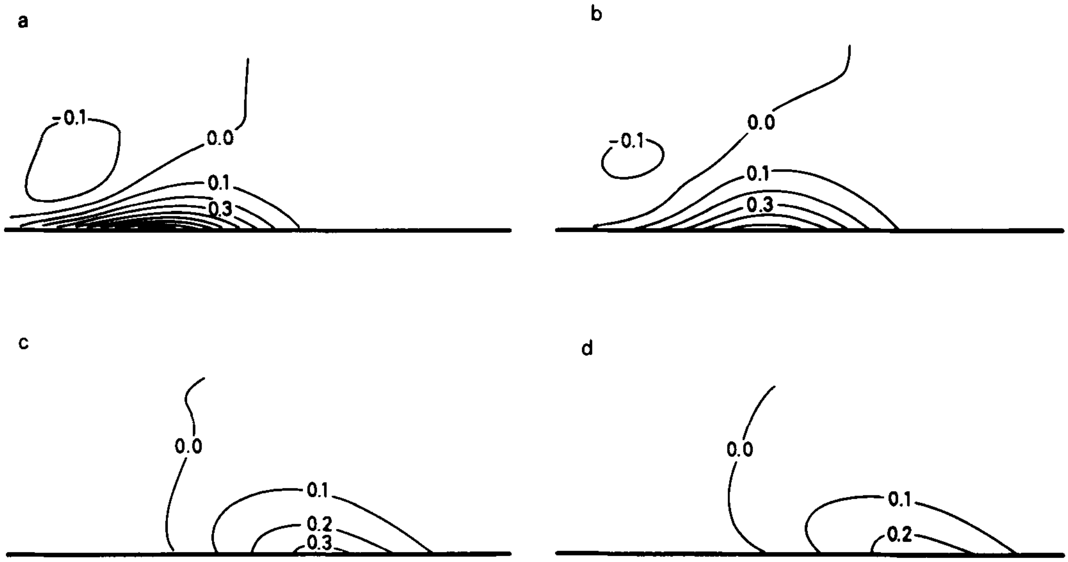

Fig. 2. (a) Isolines for surface elevation after the wind-stress (4.1) has been acting for 8 h. Equidistance 0.1 m. (b), (c) and (d) Isolines for surface elevation 4, 12 and 16 h, respectively, after the wind-stress has been switched off. Equidistance 0.1 m.

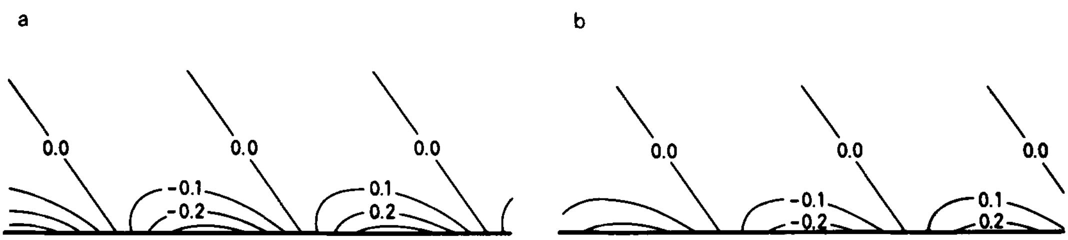

Fig. 3. Isolines for the surface elevation of a Kelvin mode. The wavelength is roughly twice the width of the free surge in Figs. 2(c) and 2(d). Equidistance 0.1 m. (a) analytical solution, (b) 4 h later.

5. Concluding remarks

The present investigation shows that friction affects internal Kelvin waves much more strongly than barotropic Kelvin waves. For given wavelength along the coast, the tilt of the co-phase lines are proportional to the product of the Coriolis parameter f and the friction parameter K_n, and inversely proportional to the square of the speed of free waves in the absence of friction. Since K_n may be of the same order, or even be larger for baroclinic waves than for barotropic, and c_n usually is much smaller, the difference in slope of the co-phase lines in the two cases may be quite considerable.

Concerning the energy of the free baroclinic Kelvin modes considered here, we note that there is no flux of energy in the direction normal to the coast. This is obvious, since v_n or V is zero. Equivalently, from (2.10); with $v_n = 0$:

$$\frac{\partial E_n}{\partial t} + \frac{\partial F_n}{\partial x} = D_n \tag{5.1}$$

where $E_n(= \frac{1}{2}u_n^2 + \frac{1}{2}c_n^2\,\zeta_n^2)$ is the energy density, $F_n(=c_n^2\,u_n\,\zeta_n)$ the energy flux along the coast and $D_n(= -K_n\,u_n^2)$ the dissipation. A similar equation is obtained for the internal mode in the two-layer case.

Internal waves of the type discussed here have been observed in fjords (Fjeldstad, 1964). The generation mechanism in that case appears to be pressure perturbations associated with tidal flow over a sill in the inlet. Unfortunately Fjeldstad did not measure the elevation or the current in the direction normal to the shore, so no information about the tilting of internal co-phase lines is available from his data.

Krauss (1978) has investigated theoretically the response of a stratified viscous sea to moving meso- and small-scale meteorological phenomena such as fronts, squall lines, gusts, etc., and concludes that these phenomena easily can produce internal waves. Although Krauss considers two-dimensional motion in an unbounded sea, there is no apparant reason why internal Kelvin waves should not be generated in the same way. It is also obvious that the generation mechanism will be particularly effective when the alongshore component of the wind field moves with a speed that is close to the speed of an internal mode.

6. Acknowledgement

During this work E. A. Martinsen was supported by the Royal Norwegian Council for Scientific and Industrial Research (NTNF) under grant 1810.7209.

REFERENCES

Bennett, J. R. 1978. A three-dimensional model of Lake Ontario summer circulation. II. A diagnostic study. *J. Phys. Oceanogr. 8*, 1095–1103.

Brink, K. H. and Allen, J. S. 1978. On the effect of bottom friction on barotropic motion over the continental shelf. *J. Phys. Oceanogr. 8*, 919–922.

Csanady, G. T. 1972. Response of large stratified lakes to wind. *J. Phys. Oceanogr. 2*, 2–13.

Defant, A. 1961. Physical Oceanography, Volume II. Pergamon Press, 598 pp.

Fjeldstad, J. E. 1929. Dynamics of free progressive tidal waves. *The Norwegian north polar expedition with the "Maud" 1918–1925*, scientific results Vol. IV. No. 3, 79 pp.

Fjeldstad, J. E. 1964. Internal waves of tidal origin. *Geofys. Publr. 25*, 5.

Gill, A. E. and Clarke, A. J. 1974. Wind induced upwelling, coastal current and sea level changes, *Deep Sea Res. 21*, 325–345.

Gjevik, B. and Røed, L. P. 1976. Storm surges along the western coast of Norway, *Tellus 28*, 166–182.

Heaps, N. S. 1969. A two-dimensional numerical sea model. *Proc. Roy. Soc., London, A 265*, 93–137.

Kraus, W. 1978. The response of stratified viscous sea to moving meteorological fronts and squall lines, *Dt. hydrogr. Z. 31*, 16–30.

Lighthill, M. J. 1969. Dynamic response of the Indian Ocean to onset of the southwest monsoon, *Phil. Trans. Roy. Soc. A, 265*, 45–92.

Martinsen, E. A., Gjevik, B. and Røed, L. P. 1979. A numerical model for long barotropic waves and storm surges along the western coast of Norway, *J. Phys. Oceanogr. 9*, 1126–1138.

Mofjeld, H. O. 1980. Effects of vertical viscosity on Kelvin waves, *J. Phys. Oceanogr. 10*, 1039–1050.

Røed, L. P. 1979. Storm surges in stratified seas. *Tellus 31*, 330–339.

Sverdrup, H. U. 1927. Dynamics of tides on the North Siberian Shelf. *Geofys. Publr. 4*, 75.

Timmerman, H. 1977. Meteorological effects on tidal heights in the North Sea. *Koninklijk Nederlands Meteorologisck Institut, mededelingen en verhandelingen No. 99*, 105 pp.

ВЛИЯНИЕ ТРЕНИЯ НА ВНУТРЕННИЕ ВОЛНЫ КЕЛЬВИНА

Теоретически исследуется влияние трения на свободные внутренние волны Кельвина. Для непрерывной стратификации трение учитывается в виде турбулентной вязкости и решения записываются в виде нормальных мод. Такая формулировка предполагает отсутствие трения о дно. Для получения аналитического решения мы предположили, что вертикальное изменение турбулентной вязкости обратно пропорционально частоте Брента-Вяйсяля. Рассматриваются как береговые, так и экваториальные волны Кельвина. Влияние трения о дно и торможение из-за трения на поверхности раздела изучаются явным образом в вертикально проинтегрированной двухслойной модели, причем сдвиговое напряжение на границе считается пропорциональным разности скоростей на ней. Формально случай непрерывной стратификации и двухслойная модель дают одинаковую систему уравнений. Даны явные формулы для затухания (амплитуд волн) из-за трения со временем, радиуса деформации Россби, частот, разности фаз между скоростью и возвышением, отклонений назад от берега внутренних поверхностей постоянной фазы. В частности показано, что последний эффект гораздо более сильный для бароклинных волн, чем для баротропной моды с той же длиной волны.